J. Civil Eng. Mater.App. 2021 (September); 5(3): 139-150

Journal of Civil Engineering and Materials Application
Journal home page: https://jcema.com

Received: 15 July 2021 • Accepted: 04 September 2021

Research

doi: 10.22034/jcema.2021.304981.1064

Structural Analysis of GFRP Elastic Gridshell Structures by Particle Swarm Optimization and Least Square Support Vector Machine Algorithms

Soheila Kookalani[1*], Bin Cheng[2]

[1]Department of Civil Engineering, Shanghai Jiao Tong University, Shanghai 200240, China.
[2]State Key Laboratory of Ocean Engineering, Shanghai Key Laboratory for Digital Maintenance of Buildings and Infrastructure, Department of Civil Engineering, Shanghai Jiao Tong University, Shanghai 200240, China.

*Correspondence should be addressed to Soheila Kookalani, Department of Civil Engineering, Shanghai Jiao Tong University, Shanghai 200240, China. Tel: +86152518327; Fax: +86152518327; Email: soheila_kookalani@sjtu.edu.cn

ABSTRACT

The gridshell structure is a kind of freeform structure, which is formed by the deformation of a flat grid and the final shape is a double curvature structure. The structural performance of the gridshell is usually obtained by finite element analysis (FEA), which is a time-consuming procedure. This paper aims to present a framework for structural analysis based on the machine learning (ML) model in order to reduce computational time. To this aim, design parameters including the length, width, height, and grid size of the structure are taken into consideration as inputs. The outputs are the member-stresses and the ratio of displacement to self-weight. Therefore, a combination of two algorithms, least-square support vector machine (LSSVM) and particle swarm optimization (PSO), is considered. PSO-LSSVM hybrid model is applied to predict the results of the structural analysis rather than the FEA. The results show that the proposed hybrid approach is an efficient method for obtaining structural performance.

Keywords: Particle swarm optimization, Support vector machine, Machine learning, Gridshell structure, Structural analysis

Copyright © 2021 Soheila Kookalani. This is an open access paper distributed under the Creative Commons Attribution License. *Journal of Civil Engineering and Materials Application* is published by *Pendar Pub*; Journal p-ISSN 2676-332X; Journal e-ISSN 2588-2880.

1.INTRODUCTION

Gridshell is a kind of spatial structure that covers large spans with the minimum amount of materials. Elastic gridshell structures have the potential to create different shapes of double-curvature structures. Structural damage reduction is an important concern for curvature structures. Thus, the structural analysis procedure is crucial for preventing structural damages. Several studies on gridshell have shown innovative strategies for designing gridshell structures (1–8). Researchers have conducted several studies in the field of gridshell structural analysis. Du Peloux et al. (9) employed the structural analysis for finding the shape in equilibrium and assess its strength, stability, and stiffness. According to the research on investigated examples, the impact of gravity and residual forces on created structures can be ignored (10). A posteriori simulation can be used to determine the effective mechanical response of the structure. Bouhaya (11) and Baverel et al. (10) demonstrated such formulations. Dimcic (5,12) developed gridshell structure optimization to achieve a stable and statically efficient grid structure. It was discovered that the combination of FEA and design process in an iterative approach might significantly decrease the gridshell structural stresses, displacements, and material of the structure, while enhancing the stability. Mesnil (13) implemented FEA in order to decrease the displacement and buckling load of the gridshells. The support vector machine (SVM) (14) and its developed version, least squares-SVM (LS-SVM) (15), are well-known artificial intelligence (AI) approaches for nonlinear function estimation in civil engineering (16). They have been utilized for calculating risk levels for bridge maintenance (17), predicting the shear strength of slabs and RC beams (18–20), predicting the backbone curve of RC rectangular columns (21), estimating the compressive strength of concrete, and approximating the resilient modulus of soil (22). The main purpose of this paper is to improve a framework for structural analysis of GFRP elastic gridshell structures. This goal is achieved using the ML technique. The design variables such as height, width in the transversal *x*-direction, length in the longitudinal *y*-direction, and grid size are considered as inputs. A hybrid method consisting of PSO and LSSVM is developed for this purpose. The LSSVM-PSO is implemented to predict the outputs. Since the FEA is a time-consuming procedure, mainly when used with the iterative process, the LSSVM method can be used instead of the FEA to reduce the required computation time. The sections of this study are arranged as follows: In the second part of this paper, the problem definition of the gridshell structural analysis is presented. Then a method for generating a variation of the structural shapes based on specific parameters is introduced in Section 3.1. Section 3.2 discusses the FEA for analyzing gridshell structures. Section 3.3 and 3.4 explain the LSSVM and PSO methods with their associated formula, respectively. Section 3.5 explains the PSO-LSSVM and demonstrates the flowchart of the process. The performance indices are presented in Section 3.6. Section 4 describes the numerical examples and the results. Finally, the conclusion is proposed in Section 5.

2. MATERIALS AND METHODS

2.1. PROBLEM DEFINITION

The first step for generating the structural shapes is to specify the design variables for the structural formation. The valid parameters for designing the shape of the gridshell are height, width in the transversal x-direction, length in the longitudinal y-direction, and grid size, as shown in Table 1. H1, H2, H3 are the height of the structure; D1, D2, D3 are the width along x-direction; S and G are the span along y-direction and the grid size, respectively. These variables act as the design variables for generating several forms. This paper aims to predict the structural performance by a hybrid ML model. The first output is the stress within the elements. In gridshell structure, the stress is associated with the curvature of beams, and the curvature is mainly caused by the shape of the gridshell (23). The breakage occurs in the elements that are overstressed. Thus, controlling the stress of the beam is essential to overcome this drawback. To this aim, Von Mises stress (σv) in the gridshell structure could be defined as follows:

$$\sigma_x = \frac{F_x}{A} \pm \frac{M_y}{W_y} \pm \frac{M_z}{W_z} \quad (1)$$

$$\tau_y = \frac{F_y}{A} \quad (2)$$

$$\tau_z = \frac{F_z}{A} \quad (3)$$

$$F_1(x) = \sigma_{v\,\max} = \left(\sqrt{\sigma_x^2 + 3\tau_y^2 + 3\tau_x^2}\right)_{\max} \quad (4)$$

Another output is the ratio of displacement to the self-weight the total weight of the gridshell is calculated as:

$$W = \sum_{i=1}^{k} \rho A_i l_i \quad (5)$$

Where ρ indicates the density of members, A_i refers to the cross-section, and l_i denotes the length of member-*i*. The equation for calculating the displacement of node-*i* is:

$$d_i = \sqrt{x_i^2 + y_i^2 + z_i^2} \quad (6)$$

Where x_i, y_i, z_i are the displacements in x, y, z directions, respectively. Accordingly, the second objective function can be expressed as follows:

$$F_2(x) = \frac{d_{i\,max}}{W} \tag{7}$$

Where d_{imax} refers to the maximum nodal displacement in the structure.

2.2. SHAPE GENERATION OF GRIDSHELL STRUCTURES

The parametric design method allows generating options, discovering trends, running simulations, adjusting variables, filtering the search, and a variety of related actions (24). This method, as an appropriate approach for designing the structure by varying the input values of the variables, is applied to create different shapes of gridshell. The values of the design variables are first identified to generate continuous shells. In the next step, the grid is generated on those surfaces with different sizes by tracing a grid on the target shape using the compass, called compass method. In this method, two guided curves are defined on the surface, and thus, the surface is divided into four parts. Then, two half-curves are divided based on the desired length of the mesh size. After that, three corners of one equilateral face can be obtained, one is the intersection of those two curves, and two others are the first segments on each curve, which are created in the last step. Later, the fourth point can be obtained by the intersection of two circles with the centers of the first segments, and the radiuses are equal to the length of the mesh size. The other three parts can be meshed by applying the same process (25). According to this criterion, changing the amount of the input variables can create different shapes. Afterward, the mesh is generated on these shapes by the mentioned method. In this regard, three generated shapes by this method are presented in Table 1.

Table 1. Design variables of the gridshell and the generated samples.

H_1	H_2	H_3	D_1	D_2	D_3	S	G
			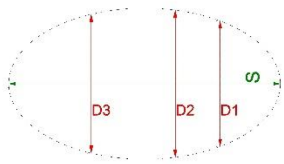			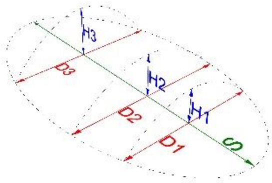	
7	**5**	**5**	**16**	**18**	**18**	**35**	**0.5**
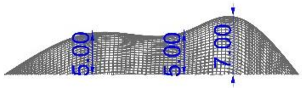			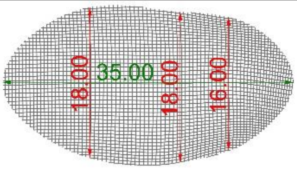			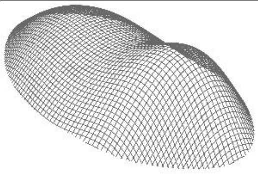	
7	**7**	**6**	**16**	**17**	**18**	**33**	**1.3**
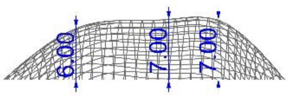			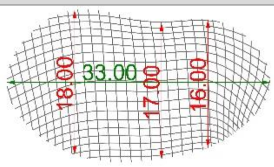			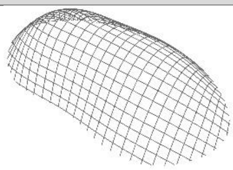	
4	**5**	**7**	**14**	**17**	**16**	**36**	**3**
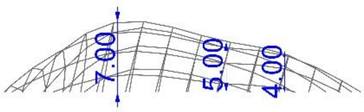			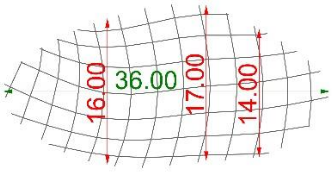			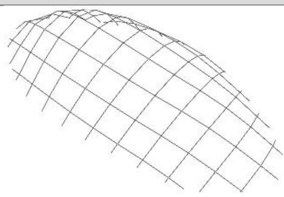	

2.3. FINITE ELEMENT MODEL

Several structural analyses performed by FEA are required for preparing the dataset. The first step is creating the 3D model of the structure that is consisted of the beam elements in *x* and *y*-direction. Afterward, the FEA conducted in the Abaqus program begins by assigning material and cross-sectional properties to the beam elements (26,27). The material should be defined based on its mechanical properties. Glass fiber reinforcement polymer (GFRP) is a type of composite material, which can significantly improve the bearing capacity and stiffness of gridshell structures, thanks to its high strength, elastic limit strain, and young's modulus (28). The mechanical properties of GFRP are shown in Table 2.

Table 2. Mechanical properties of GFRP (23).

Tube	Exp. strength R (mean value)	Exp. coefficient of variation C_v	Strength (com. data)	Coefficient of variation (com. data)
GFRP pultruded	480 MPa	3%	440 MPa	Not disclosed

The bending test of GFRP tubes demonstrated linear behavior before their breakage (29); thus, the linear elastic constitutive model is defined in the FEA for the beam elements. GFRP is commonly used for constructing the elastic gridshell in the form of the circular pultruded tube that should be considered for simulation. Therefore, the structural elements of the gridshells are described as circular GFRP tubes with Young's modulus (E) of 26 GPa and density (d) of 1850 kg/m3. The structural members are simulated by the beam element B32; therefore, the axial forces, shear, and bending moments of the gridshell may be precisely computed. Furthermore, the swivel scaffold connectors are utilized to simulate the connections. The swivel scaffold connection prohibits the out-of-plane rotations and the translations between the nodes, while allowing in-plane rotation. Fixed supports are established for the beam ends to prevent translations and rotations. The structural self-weight is defined as the gravitational acceleration of 9.8 N/kg, and the weight of equipment is assumed to be 2 kN/m^2.

2.4. LEAST SQUARE SUPPORT VECTOR MACHINE (LSSVM)

Suykens and Vandewalle (30) presented the LSSVM that offers a computational advantage in comparison with the SVM by converting the inequality constraints of the Quadratic Programming (QP) problem into a system of linear equations, resulting in faster calculations and lower computational complexity (31,32). The constraint problem is transformed into an unconstrained problem by introducing Lagrange multipliers in the low-dimensional feature space. Then, the kernel function projects the problem to a high-dimensional feature space. The kernel function can simplify the computation of linearly non-separable issues. Besides, adjusting the parameters of the kernel function leads to changing the dimensions of the LSSVM feature space in order to achieve maximum accuracy and minimum error. The LSSVM optimization problem can be expressed as follows:

$$\min J(w,b,\xi)=\frac{1}{2}\|w\|^2+\frac{1}{2}\gamma\sum_{i=1}^{n}\xi_i^2 \quad (8)$$

The following constraints are applied to the above equation:

$$y_i\left[w^T\phi(x_i)+b\right]=1-\xi_i,\ i=1,2,3,\ldots,n \quad (9)$$

Where $b\in R$ refers to a bias term, and w represents the weight vector. Furthermore, ξ_i denotes a slack variable that indicates how far a data deviates from the ideal condition, and γ indicates a regularization factor. As previously stated, Lagrange multipliers a_i (i=1, 2, 3, …, n) are used to address the optimization problems more efficiently. The Lagrange function is created as:

$$L(w,b,\xi,a)=\frac{1}{2}\|w\|^2+\frac{1}{2}\gamma\sum_{i=1}^{n}\xi_i^2-\sum_{i=1}^{n}a_i\left\{y_i\left[w^T\phi(x_i)+b\right]-1+\xi_i\right\} \quad (10)$$

The kernel function selection problem is the first issue that must be solved when implementing the LSSVM. Model learning performance is influenced by the kernel function parameters. The radial basis function (RBF), which has fewer parameters than a polynomial kernel function, is one f the most effective kernel functions. The expression of RBF is as follows:

$$K(x, x_i) = \exp\left(-\frac{\|x - x_i\|}{\sigma^2}\right) \quad (11)$$

Where, σ^2 indicates the parameters of the kernel function. The regularization parameter γ and values of the kernel function parameter σ^2 have a great influence on the performance of the LSSVM model. The distribution of the data after mapping to the new feature space is implicitly determined by the kernel parameter σ^2. The regularization parameter γ is utilized to modify the ratio between the empirical risk and confidence range; thus, the structural risk is minimized (33).

2.5. PARTICLE SWARM OPTIMIZATION (PSO)

In this study, PSO is implemented for the parameters optimization of LSSVM. PSO is a population-based search approach. Particles in the population are impacted by self- and social-cognition, and subsequently, update their velocities and locations using Eqs. (12) and (13). Finally, each particle moves towards the optimal location.

$$v_{id}(t+1) = wv_{id}(t) + c_1 r_1(t)\left(p_{id}(t) - x_{id}(t)\right) + c_2 r_2(t)\left(p_{gd}(t) - x_{id}(t)\right) \quad (12)$$

$$x_{id}(t+1) = x_{id}(t) + v_{id}(t+1) \quad (13)$$

where, i=1,2,…,N, N denotes the number of particles; the subscript d demonstrates the dimension of a particle; t refers to the number of iterations; $p_{id}(t)$ indicates the optimal position of the i^{th} particle; and $p_{gd}(t)$ is the optimal location. c_1 and c_2 are acceleration coefficients; w is the inertia weight as bellow:

$$w = w_{max} - (w_{max} - w_{min})\frac{t}{t_{max}} \quad (14)$$

where, w_{max} and w_{min} represent the maximum and minimum inertia factors, respectively; t_{max} indicates the maximum amount of iterations. The PSO method can tackle global optimal solution issues with a simple structure, quick convergence, and broad search range. The particle group has memory during the procedure of target problem optimization, and particles can pass the best locations of particle history to each other. Moreover, there are no complicated mathematical procedures like mutation and crossover, and no need to establish a lot of sophisticated parameters. Currently, the PSO technique has been expanded to the larger domains (34), such as neural network and pattern recognition training. Another major development trend is integration with other intelligent algorithms (35).

2.6. PSO-LSSVM MODEL

PSO-LSSVM model is established to optimize the parameters of LSSVM. The particle fitness function and the representation of the parameters must be taken into account during the optimization. The fitness is utilized to determine the location of particles. The more robust adaptability is achieved by the smaller fitness function. In this study, the fitness function is the mean square error (MSE) of the training samples and is expressed as:

$$\Delta e = \frac{1}{N}\sum_{i=1}^{N}(y_{ib} - y'_{ib})^2 \quad (15)$$

Where, y_{ib} and y'_{ib} denote the actual and prediction labels of the training samples, respectively. The iterative process requires a nonlinear FEA in each iteration that is a time-consuming procedure. Consequently, the LSSVM, as a surrogate model, is utilized for structural performance prediction in order to reduce the required time. To this aim, this model is attempted by splitting the dataset into training and testing data.

The steps of the PSO-LSSVM model are as follows (36):
Step1: Import data and split it into training and testing sets.
Step2: Optimization of parameters.
Step2.1: Set the size of the swarm, maximum number of iterations, velocities, and positions of the particles.
Step2.2: Build LSSVM models and calculate the MSE.
Step2.3: Assess the fitness of each particle.

Step2.4: Update the global optimal solution p_{gd} and the individual extremum p_{id}. Update the p_{id}, if the fitness of the particle is less than the initial individual extremum. Otherwise, retrain the same values. Obtain the p_{gd} on the basis of the fitness of each particle.
Step2.5: Update the velocity, location, and inertia weight.
Step2.6: Steps 2.2–2.6 should be repeated until a termination condition is fulfilled.
Step2.7: Obtain the optimal parameters.
Step3: Implement the LSSVM model with obtained parameters
The overall procedure has two significant parts; simulation and analysis of samples and utilizing the combination of PSO and LSSVM for accurate prediction, as shown in Figure 1.

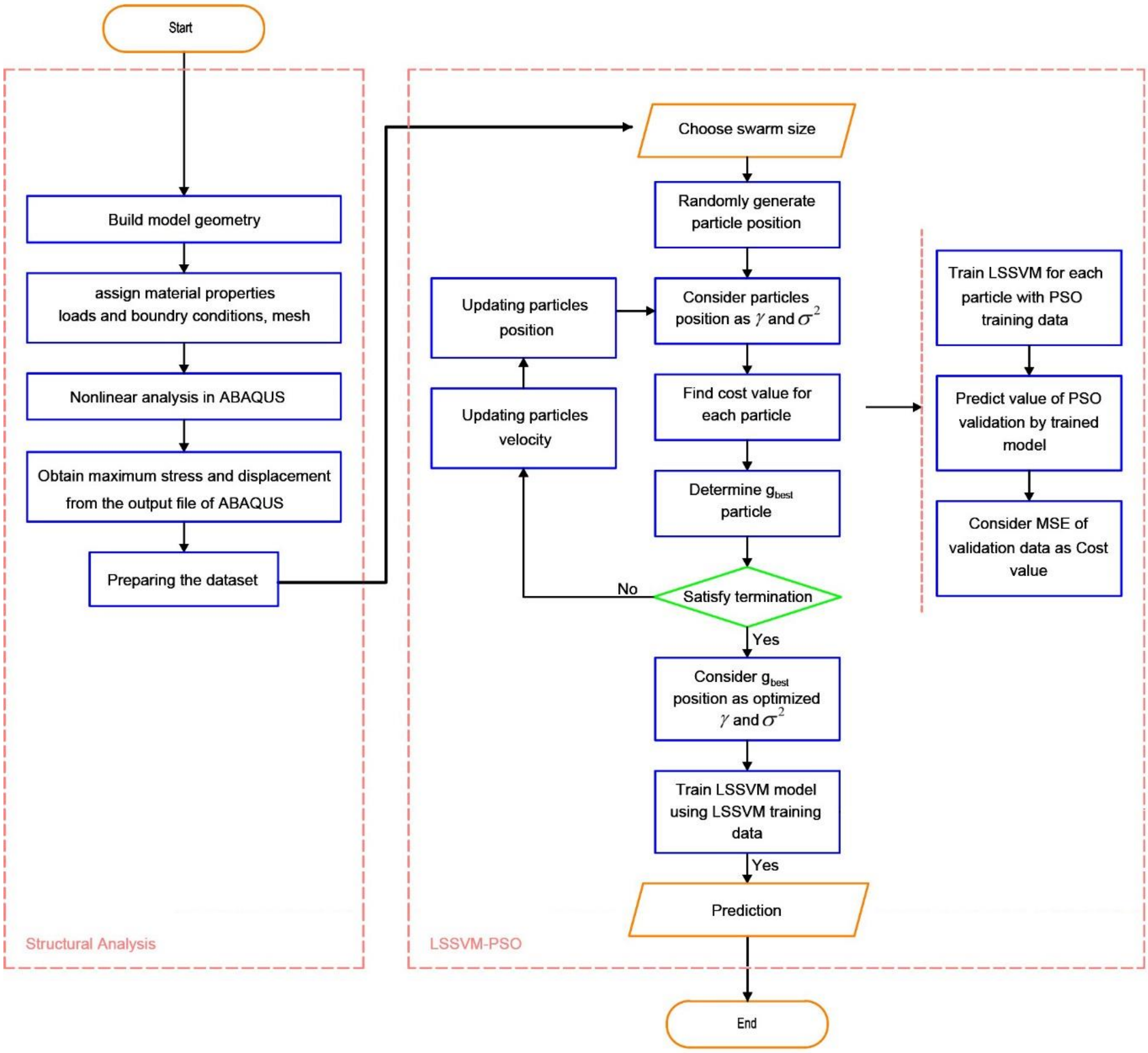

Figure 1. Flowchart of the structural performance estimation process.

2.7. PERFORMANCE INDICES

Root mean square error (RMSE) and the normalized mean square error (NMSE) are utilized as performance indices for the ML model (37), which are formulated as follows:

$$RMSE = \sqrt{\frac{1}{n}\sum_{i=1}^{n}(y_i - \hat{y}_i)^2} \quad (16)$$

$$NMSE = \frac{1}{\delta^2 n}\sum_{i=1}^{n}(y_i - \hat{y}_i)^2, \delta^2 = \frac{1}{n-1}\sum_{i=1}^{n}(y_i - \bar{y})^2 \quad (17)$$

Where n is the number of data in the test-set and $y_i, \hat{y}_i, \bar{y}_i$ are actual, predicted, and the mean of the actual values, respectively.

2.8. NUMERICAL EXAMPLE

The goal of the case study is to establish a hybrid ML model for predicting the outputs with high accuracy. To this aim, the upper and lower bounds of each design parameter are defined for generating different shapes that are shown in Table 3.

Table 3. Lower and upper bounds of the design variables.

Parameter	H_1	H_2	H_3	D_1	D_2	D_3	S	G
Lower bound (m)	**4**	**5**	**4**	**14**	**14**	**16**	**32**	**0.5**
Upper bound (m)	**8**	**7**	**8**	**18**	**22**	**20**	**37**	**3**

Afterward, a wide variety of geometries comprising 160 samples are generated by the mentioned method, as shown in Figure 2.

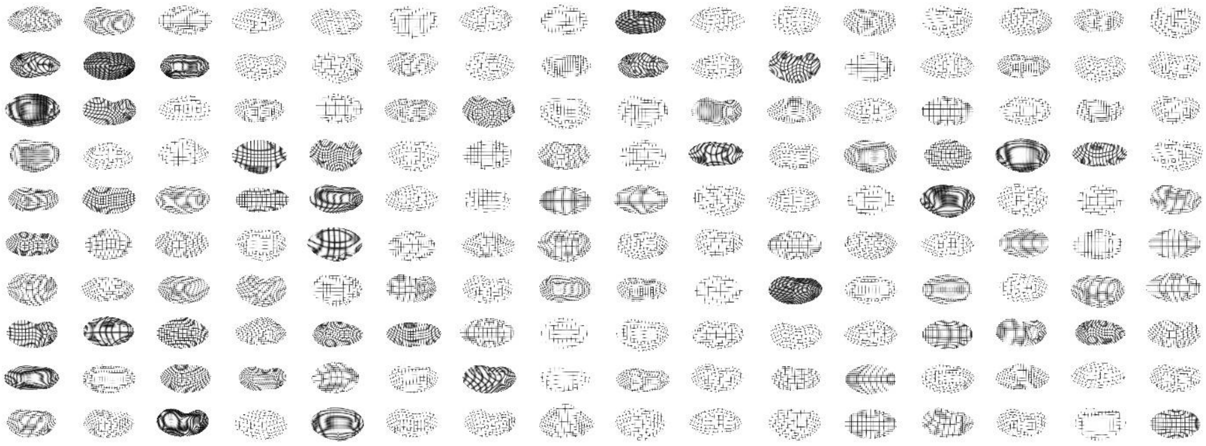

Figure 2. Shape generation of GFRP elastic gridshell structure.

Figure 3 demonstrates the stresses and displacements within the sections of all meshed members in an analyzed sample. The structure covers an area of about 528 m^2 with the weight of 8.04 kN. The first output is equal to 13.1 MPa and the second output is equal to 2.95 mm/kN.

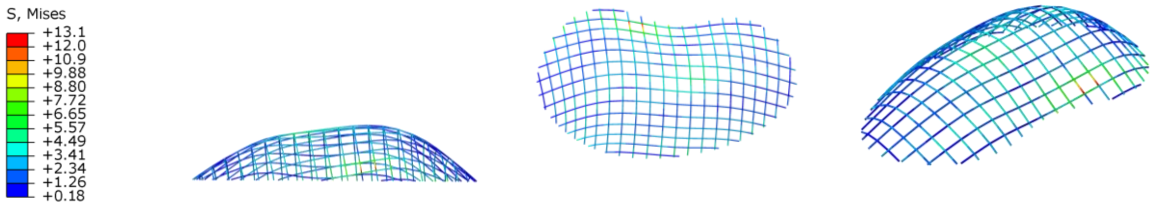

(a) H_1=5, H_2=6, H_3=6, D_1=17, D_2=17, D_3=19, S=34, G=1.8; Maximum stress=13.1 MPa

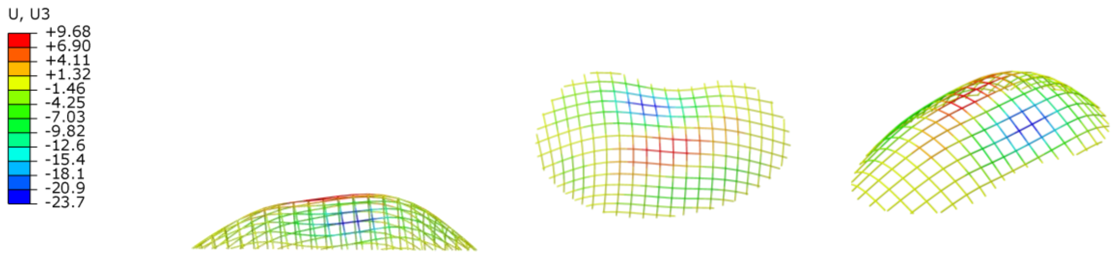

(b) H_1=5, H_2=6, H_3=6, D_1=17, D_2=17, D3=19, S=34, G=1.8; Maximum displacement/W=2.95 mm/kN

Figure 3. Structural analysis of GFRP elastic gridshell: (a) Stress (MPa); (b) Displacement (mm/kN).

Figure 4 depicts the structural performance includes the stresses of all the elements, and displacement of all the nodes.

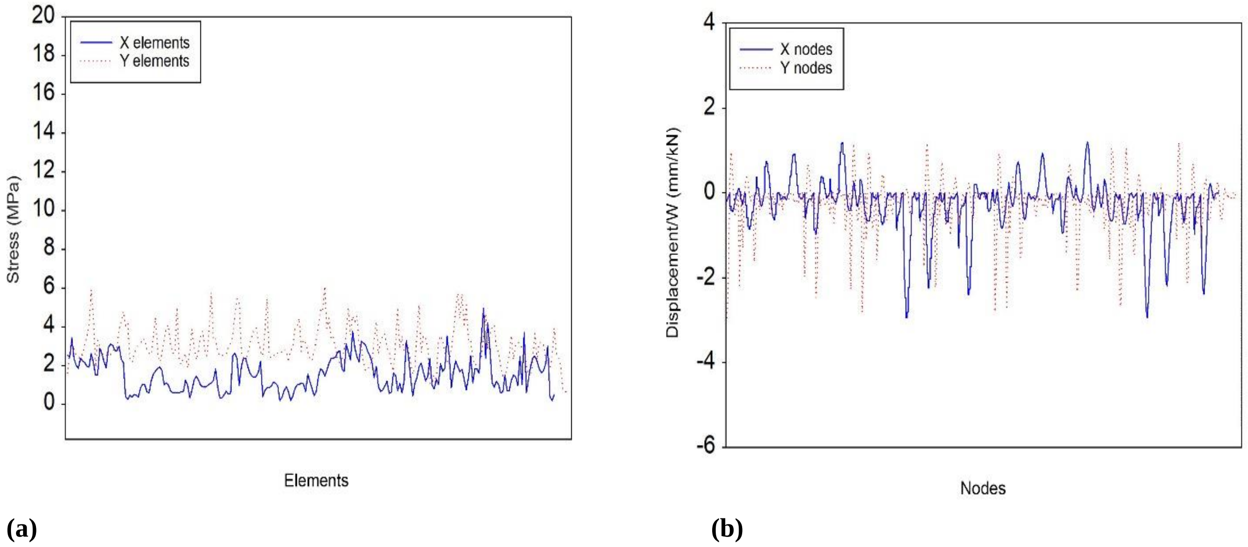

Figure 4. Structural performance of gridshell: (a) Stress (MPa); (b) Displacement/W (mm/kN).

The next step is using the generated dataset to train the LSSVM model for predicting the estimated performance of the structure, during which the PSO is carried out simultaneously to increase the accuracy. For this purpose, the extracted dataset from the FEA, including 160 samples, is divided into two parts with about 0.8 training set ratio; 130 training and 30 testing models.

3. RESULTS AND DISCCUSION

Setting the parameters of PSO, including cognitive constant (C_1), social constant (C_2), inertial weight (*w*), number of particles, and number of iterations, is the first step of the procedure. Sixteen combinations of these parameters have been defined in Table 4. Both cognitive and social coefficients are considered equal to 0.5, 1, 1.5, and 2. The inertial weight is increased from 0.2 to 0.9. Population size is set to be 10, 50, and 100 for the iteration number of 500, 300, and 100. Subsequently, RMSE and NMSE as performance functions in the testing model related to both objective functions and σ^2 and γ as the parameters of LSSVM are presented in Table 5 and Table 6. Obviously, the lower values of these two indicators lead to more accurate results.

Table 4. Different values of the parameters of PSO algorithm.

Case	C_1	C_2	*w*	Size pop	Iteration
1	0.5	0.5	0.2	10	500
2	1	0.5	0.5	50	300
3	1.5	0.5	0.9	100	100
4	2	0.5	0.2	10	500
5	0.5	1	0.5	50	300
6	1	1	0.9	100	100
7	1.5	1	0.2	10	500
8	2	1	0.5	50	300
9	0.5	1.5	0.9	100	100
10	1	1.5	0.2	10	500
11	1.5	1.5	0.5	50	300
12	2	1.5	0.9	100	100
13	0.5	2	0.2	10	500
14	1	2	0.5	50	300
15	1.5	2	0.9	100	100
16	2	2	0.2	10	500

Table 5. Performance indexes and optimal parameters of the LSSVM model for the output 1.

Case	NMSE	RMSE	σ^2_1	γ_1
1	0.2036	0.000960	4.2834	1.0772
2	0.0624	0.000531	0.0652	5.6224
3	0.0697	0.000561	0.0122	19.5375
4	0.2062	0.000966	4.3313	1.0491
5	0.0746	0.000581	0.0108	100
6	0.0850	0.000620	0.0100	83.6764
7	0.1707	0.000879	3.6038	1.5864
8	0.0746	0.000581	0.0108	100
9	0.0847	0.000619	0.0100	92.3259
10	0.0846	0.000618	0.0100	100
11	0.0846	0.000618	0.0100	100
12	0.0848	0.000619	0.0100	89.9708
13	0.0846	0.000618	0.0100	100
14	0.0846	0.000618	0.0100	100
15	0.0847	0.000619	0.0100	94.1816
16	0.0846	0.000618	0.0100	100

Table 6. Performance indexes and optimal parameters of the LSSVM model for the output 2.

Case	NMSE	RMSE	σ^2_2	$_2\gamma$
1	0.0332	0.000507	2.3706	1.2117
2	0.0065	0.000224	1.5628	4.8317
3	0.0307	0.000487	0.0134	21.7702
4	0.0395	0.000552	2.4863	1.0655
5	0.0344	0.000515	0.0118	100
6	0.0535	0.000643	0.0100	83.6085
7	0.0237	0.000428	2.1709	1.5646
8	0.0344	0.000515	0.0118	100
9	0.0533	0.000642	0.0100	93.5243
10	0.0531	0.000641	0.0100	100
11	0.0344	0.000515	0.0118	100
12	0.0534	0.000642	0.0100	90.0427
13	0.0344	0.000515	0.0118	100
14	0.0531	0.000641	0.0100	100
15	0.0532	0.000642	0.0100	94.3549
16	0.0344	0.000515	0.0118	100

As can be seen in Table 5 and Table 6, Case 2 demonstrates the best performance. Thus, the PSO algorithm with C_1=1, C_2=0.5, w=0.5, 50 particles, and 300 iterations is applied for more accurate prediction. Consequently, the parameters for the first output equal 0.0652 and 5.6224, and for the second output are set to be 1.5628 and 4.8317. The actual values of the train and test data and the predicted amount are compared in Figure 5 and Figure 6, which verify the prediction accuracy.

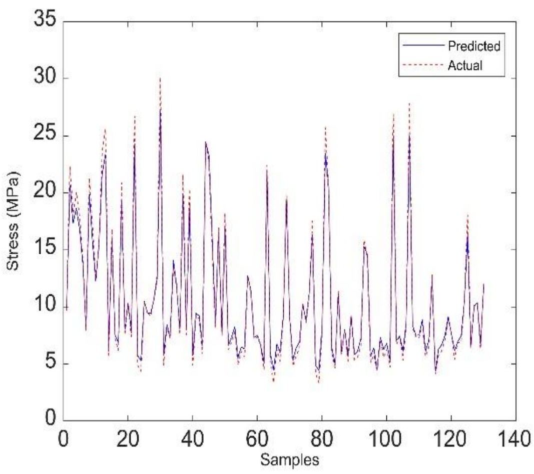

(a)

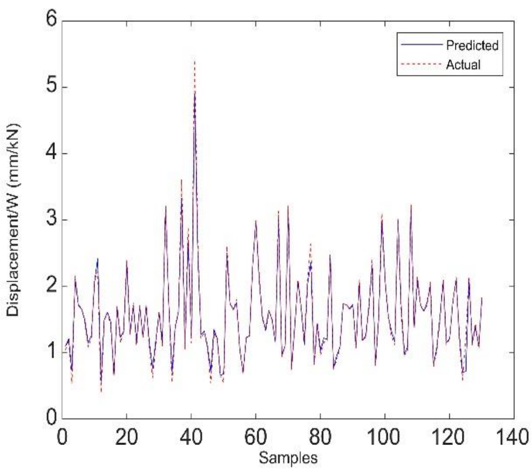

(b)

Figure 5. Comparison of the actual and predicted value of train data for outputs: (a) Maximum Stress (MPa); (b) Maximum Displacement/Self-weight (mm/kN).

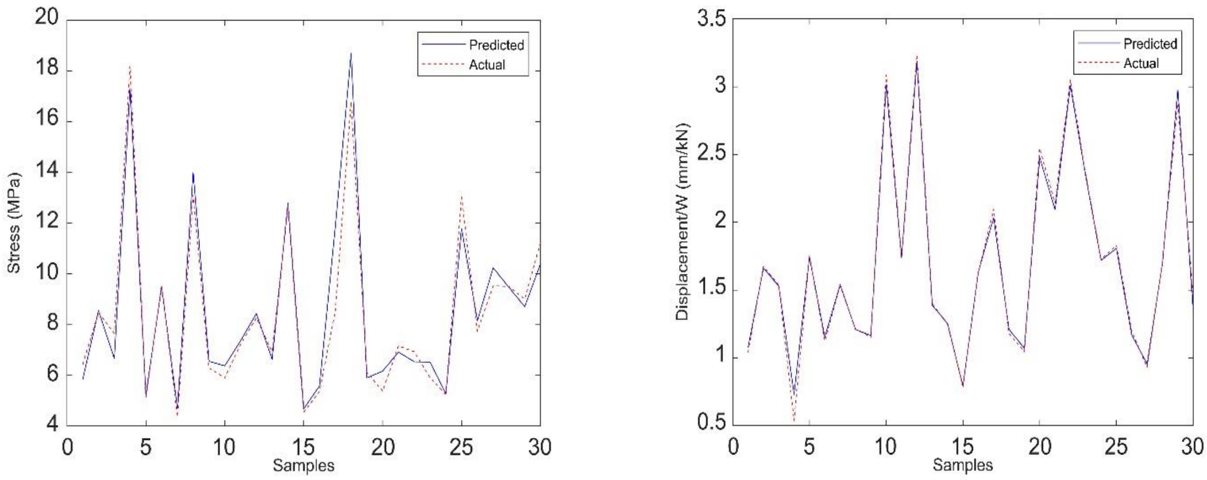

(a) (b)

Figure 6. Comparison of the actual and predicted value of test data for outputs: (a) Maximum Stress (MPa); (b) Maximum Displacement/Self-weight (mm/kN).

Table 7 and Table 8 present the comparison of measured and predicted values of outputs. It is verified from the numerical results that the prediction of the second output is more accurate compared to the first one, while for both, it is accurate enough.

Table 7. Comparison of maximum stress (MPa) measured and predicted at the test-set.

Case	1	2	3	4	5	6
Measured	6.44	8.47	7.67	18.20	5.14	9.58
Predicted	5.84	8.55	6.67	17.30	5.23	9.49
Case	7	8	9	10	11	12
Measured	4.38	13.10	6.29	5.91	7.23	8.27
Predicted	4.72	14.00	6.56	6.38	7.37	8.44
Case	13	14	15	16	17	18
Measured	6.93	12.7	4.55	5.37	8.53	16.80
Predicted	6.63	12.80	4.68	5.59	11.90	18.70
Case	19	20	21	22	23	24
Measured	6.13	5.39	7.17	6.94	5.92	5.25
Predicted	5.91	6.17	6.92	6.54	6.53	5.28
Case	25	26	27	28	29	30
Measured	13.00	7.75	9.53	9.51	9.01	11.30
Predicted	11.80	8.16	10.2	9.47	8.71	10.4

Table 8. Comparison of maximum displacement/self-weight (mm/kN) measured and predicted at the test-set.

Case	1	2	3	4	5	6
Measured	1.04	1.67	1.54	0.53	1.75	1.12
Predicted	1.08	1.66	1.53	0.73	1.74	1.15
Case	7	8	9	10	11	12
Measured	1.53	1.21	1.15	3.09	1.74	3.23
Predicted	1.54	1.21	1.17	3.02	1.74	3.19
Case	13	14	15	16	17	18
Measured	1.40	1.25	0.79	1.63	2.10	1.18
Predicted	1.39	1.25	0.78	1.63	2.03	1.21
Case	19	20	21	22	23	24
Measured	1.05	2.55	2.14	3.05	2.36	1.73
Predicted	1.07	2.48	2.09	3.01	2.34	1.72
Case	25	26	27	28	29	30
Measured	1.83	1.20	0.92	1.17	2.88	1.44
Predicted	1.81	1.17	0.95	1.70	2.98	1.35

The presented results reveal that the proposed method significantly reduces the required time for the analysis process and can be used as an effective and fast procedure to analyze the gridshell structure.

4. CONCLUSION

This paper proposes a structural performance prediction approach for GFRP elastic gridshell structures using a hybrid ML model. Design parameters including height, width in the transversal *x*-direction, length in the longitudinal *y*-direction, and the grid size are considered as input variables. The maximum stress denotes the first output, and the ratio of displacement to self-weight is adopted as the second output. Several FEA are performed to provide the dataset for the ML algorithm. A method combining the LSSVM and PSO is proposed for predicting structural performance. In summary, the PSO-LSSVM with a low error rate is able to predict the structural performance of structures, which effectively reduces the computational time compared to the FEA. The presented hybrid approach is proved to be an efficient tool for the analysis of elastic gridshell structures. Generally, the proposed hybrid method can be implemented in any structure made of beams and demonstrates efficient results in accuracy and computational time in comparison with the FEA.

FUNDING/SUPPORT

Not mentioned any Funding/Support by authors.

ACKNOWLEDGMENT

Not mentioned by authors.

AUTHORS CONTRIBUTION

This work was carried out in collaboration among all authors.

CONFLICT OF INTEREST

The author (s) declared no potential conflicts of interests with respect to the authorship and/or publication of this paper.

5. REFRENCES

[1] Richardson JN, Adriaenssens S, Coelho RF, Bouillard P. Coupled form-finding and grid optimization approach for single layer grid shells. Engineering structures. 2013 Jul 1;52:230-9. [View at Google Scholar]; [View at Publisher].

[2] Bouhaya L, Baverel O, Caron JF. Optimization of gridshell bar orientation using a simplified genetic approach. Structural and Multidisciplinary Optimization. 2014 Nov 1;50(5):839-48. [View at Google Scholar]; [View at Publisher].

[3] Adriaenssens S, Block P, Veenendaal D, Williams C, editors. Shell structures for architecture: form finding and optimization. Routledge; 2014 Mar 21. [View at Google Scholar]; [View at Publisher].

[4] D'Amico B, Kermani A, Zhang H. Form finding and structural analysis of actively bent timber grid shells. Engineering Structures. 2014 Dec 15;81:195-207. [View at Google Scholar]; [View at Publisher].

[5] Dimcic M. Structural Optimization of Grid Shells Based on Genetic Algorithms. Ph.D Thesis. 2011. [View at Google Scholar]; [View at Publisher].

[6] Dini M, Estrada G, Froli M, Baldassini N. Form-finding and buckling optimisation of gridshells using genetic algorithms. InProceedings of IASS Annual Symposia 2013 Sep 27 (Vol. 2013, No. 16, pp. 1-6). International Association for Shell and Spatial Structures (IASS). [View at Google Scholar]; [View at Publisher].

[7] Douthe C, Baverel O, Caron JF. Form-finding of a grid shell in composite materials. Journal of the International Association for Shell and Spatial structures. 2006 Apr 1;47(1):53-62. [View at Google Scholar]; [View at Publisher].

[8] Kookalani S, Cheng B, Xiang S. Shape optimization of GFRP elastic gridshells by the weighted Lagrange ε-twin support vector machine and multi-objective particle swarm optimization algorithm considering structural weight. InStructures 2021 Oct 1 (Vol. 33, pp. 2066-2084). Elsevier. [View at Google Scholar]; [View at Publisher].

[9] Du Peloux L, Baverel O, Caron JF, Tayeb F. From shape to shell: a design tool to materialize freeform shapes using gridshell structures. InDesign Modelling Symposium Berlin 2013 Sep 28. [View at Google Scholar]; [View at Publisher].

[10] Baverel O, Caron JF, Tayeb F, Du Peloux L. Gridshells in composite materials: construction of a 300 m2 forum for the solidays' festival in Paris. Structural engineering international. 2012 Aug 1;22(3):408-14. [View at Google Scholar]; [View at Publisher].

[11] Bouhaya L. Structural optimization of gridshells. PhD thesis, Universit´e Paris-Est; 2010. [View at Publisher].

[12] Dimcic M, Knippers J. Free-form grid shell design based on genetic algorithms. In: Integration Through Computation - Proceedings of the 31st Annual Conference of the Association for Computer Aided Design in Architecture, ACADIA 2011. 2011. [View at Google Scholar]; [View at Publisher].

[13] Mesnil R, Ochsendorf J, Douthe C. Influence of the pre-stress on the stability of elastic grid shells. InProceedings of IASS Annual Symposia 2013 Sep 27 (Vol. 2013, No. 4, pp. 1-5). International Association for Shell and Spatial Structures (IASS). [View at Google Scholar]; [View at Publisher].

[14] Vapnik VN. The Nature of Statistical Learning Theory. Springer-Verlag. Adaptive and learning Systems for Signal Processing, Communications and Control. 1995. [View at Google Scholar]; [View at Publisher].

[15] Suykens JA, Van Gestel T, De Brabanter J, De Moor B, Vandewalle JP. Least squares support vector machines. World scientific; 2002 Nov 12. [View at Google Scholar]; [View at Publisher].

[16] Ahmadi Maleki M, Emami M. Application of SVM for Investigation of Factors Affecting Compressive Strength and Consistency of Geopolymer Concretes. Journal of civil Engineering and Materials Application. 2019 Jun 1;3(2):101-7. [View at Google Scholar]; [View at Publisher].

[17] Cheng MY, Hoang ND. Risk score inference for bridge maintenance project using evolutionary fuzzy least squares support vector machine. Journal of Computing in Civil Engineering. 2014 May 1;28(3):04014003. [View at Google Scholar]; [View at Publisher].

[18] Chou JS, Ngo NT, Pham AD. Shear strength prediction in reinforced concrete deep beams using nature-inspired metaheuristic support vector regression. Journal of Computing in Civil Engineering. 2016 Jan 1;30(1):04015002. [View at Google Scholar] ; [View at Publisher].

[19] Pal M, Deswal S. Support vector regression based shear strength modelling of deep beams. Computers & Structures. 2011 Jul 1;89(13-14):1430-9. [View at Google Scholar]; [View at Publisher].

[20] Vu DT, Hoang ND. Punching shear capacity estimation of FRP-reinforced concrete slabs using a hybrid machine learning approach. Structure and Infrastructure Engineering. 2016 Sep 1;12(9):1153-61. [View at Google Scholar]; [View at Publisher].

[21] Luo H, Paal SG. Machine learning–based backbone curve model of reinforced concrete columns subjected to cyclic loading reversals. Journal of Computing in Civil Engineering. 2018 Sep 1;32(5):04018042. [View at Google Scholar]; [View at Publisher].

[22] Chou JS, Pham AD. Smart artificial firefly colony algorithm‐based support vector regression for enhanced forecasting in civil engineering. Computer‐Aided Civil and Infrastructure Engineering. 2015 Sep;30(9):715-32. [View at Google Scholar]; [View at Publisher].

[23] Tayeb F, Caron JF, Baverel O, Du Peloux L. Stability and robustness of a 300 m2 composite gridshell structure. Construction and Building Materials. 2013 Dec 1;49:926-38. [View at Google Scholar]; [View at Publisher].

[24] Brown NC, Jusiega V, Mueller CT. Implementing data-driven parametric building design with a flexible toolbox. Automation in Construction. 2020 Oct 1;118:103252. [View at Google Scholar]; [View at Publisher].

[25] Quinn G, Gengnagel C. A review of elastic grid shells, their erection methods and the potential use of pneumatic formwork. Mobile and rapidly assembled structures IV. 2014 Jun 11;136:129. [View at Google Scholar]; [View at Publisher].

[26] Xiang S, Cheng B, Zou L, Kookalani S. An integrated approach of form finding and construction simulation for glass fiber‐reinforced polymer elastic gridshells. The Structural Design of Tall and Special Buildings. 2020 Apr 10;29(5):e1698. [View at Google Scholar]; [View at Publisher].

[27] Xiang S, Cheng B, Kookalani S. An analytic solution for form finding of GFRP elastic gridshells during lifting construction. Composite Structures. 2020 Jul 15;244:112290. [View at Google Scholar]; [View at Publisher].

[28] Xiang S, Cheng B, Kookalani S, Zhao J. An analytic approach to predict the shape and internal forces of barrel vault elastic gridshells during lifting construction. InStructures 2021 Feb 1 (Vol. 29, pp. 628-637). Elsevier. [View at Google Scholar]; [View at Publisher].

[29] Douthe C, Caron JF, Baverel O. Gridshell structures in glass fibre reinforced polymers. Construction and building materials. 2010 Sep 1;24(9):1580-9. [View at Google Scholar]; [View at Publisher].

[30] Suykens JA, Vandewalle J. Least squares support vector machine classifiers. Neural processing letters. 1999 Jun;9(3):293-300. [View at Google Scholar]; [View at Publisher].

[31] Van Gestel T, Suykens JA, Baesens B, Viaene S, Vanthienen J, Dedene G, De Moor B, Vandewalle J. Benchmarking least squares support vector machine classifiers. Machine learning. 2004 Jan;54(1):5-32. [View at Google Scholar]; [View at Publisher].

[32] Roushangar K, Saghebian SM, Mouaze D. Predicting characteristics of dune bedforms using PSO-LSSVM. International Journal of Sediment Research. 2017 Dec 1;32(4):515-26. [View at Google Scholar]; [View at Publisher].

[33] Chamkalani A, Zendehboudi S, Bahadori A, Kharrat R, Chamkalani R, James L, Chatzis I. Integration of LSSVM technique with PSO to determine asphaltene deposition. Journal of Petroleum Science and Engineering. 2014 Dec 1;124:243-53. [View at Google Scholar]; [View at Publisher].

[34] Junior FE, Yen GG. Particle swarm optimization of deep neural networks architectures for image classification. Swarm and Evolutionary Computation. 2019 Sep 1;49:62-74. [View at Google Scholar]; [View at Publisher].

[35] Hajabdollahi H, Ahmadi P, Dincer I. Thermoeconomic optimization of a shell and tube condenser using both genetic algorithm and particle swarm. International journal of refrigeration. 2011 Jun 1;34(4):1066-76. [View at Google Scholar]; [View at Publisher].

[36] Ren Z, Han H, Cui X, Qing H, Ye H. Application of PSO-LSSVM and hybrid programming to fault diagnosis of refrigeration systems. Science and Technology for the Built Environment. 2021 May 28;27(5):592-607. [View at Google Scholar]; [View at Publisher].

[37] ISECS International Colloquium on Computing, Communication, Control, and Management. Advancing Computing, Communication, Control and Management. Luo Q, editor. Berlin: Springer; 2010. [View at Google Scholar]; [View at Publisher].